ISSN 8755-6839

SCIENCE OF TSUNAMI HAZARDS

Journal of Tsunami Society International

Volume 36 Number 3 2017

REVIEW OF EARTHQUAKES AND TSUNAMI RECORDS AND CHARACTERIZATION OF CAPABLE FAULTS ON THE NORTHWESTERN COAST OF ECUADOR

Kervin Chunga[1]*, TheofilosToulkeridis[2]*, Xavier Vera-Grunauer[3-4], Marllelis Gutierrez[1], Nestor Cahuana[4], Alamir Alvarez[1]

[1]Universidad Estatal Península Santa Elena, Facultad de Ciencias de la Ingeniería. Ecuador
[2]Universidad de las Fuerzas Armadas ESPE, Sangolquí, Quito, Ecuador.
[3]Universidad Católica de Santiago de Guayaquil, Facultad de Ingeniería, Ecuador.
[4]Geoestudios S.A., Guayaquil, Ecuador
*Corresponding authors: kchunga@upse.edu.ec; ttoulkeridis@espe.edu.ec

ABSTRACT

There are only few documented moderate to strong earthquakes associated with active tectonics of capable crustal faults in Ecuador's northwestern coastal region. The short seismic record begins with the great earthquake and tsunami on January 31, 1906 (Mw 8.8), followed by other destructive earthquakes and tsunamis in the subduction zone, which are recorded on January 19, 1958 (Mw 7.6) and December 12, 1979 (Mw 7.7). Furthermore, modest earthquakes from capable faults have been registered on April 9, 1976 (Mw 6.7), January 2, 1981 (Mw 5.9), June 25, 1989 (Mw 6.3), April 20, 2016 (Mw 6.0) and January 31, 2017 (Mw 5.5, MLv 5.7). Earthquakes of minor magnitude have not been considered in this study, as they lack to cause coseismic ground effects. In this study, a catalog of geological fault has been delineated with 41 segments of capable and active faults on the sea floor and inland segments of Esmeraldas and Manabí provinces, as the instrumental seismic record does not provide sufficient information to evaluate the seismic risk due to faults capable of generating earthquakes larger than Mw≥6. This methodological approach allowed to estimate the seismicity levels in the order of 6.0≤Mw≤7.3 and rock peak ground accelerations in the order of 0.42g 0.26g. These values have been obtained from empirical regression equations applied to the length of capable geological faults.

The seismogenic structure of the subduction zone is able to generate earthquakes and subsequently tsunamis in the order of 8.2≤Mw≤9.0, and may cause coseismic ground damage to the close-by (82km), highly-populated city of Esmeraldas. This structural geological analysis is able to provide new insights, which need to be considered in studies of seismic hazards and particularly in the generation of control spectra for vertical as well as horizontal components from capable faults.

Keywords: Earthquake and tsunami hazard, capable fault, Ecuador's northwestern coast.

1. INTRODUCTION

Regression equations applied to geometric and kinematic parameters of active and capable geological faults allow the estimation of maximum magnitudes (Wells and Coppersmith, 1994; Wesnousky, 2008; Leonard, 2010; Stirling et al., 2013) as well as Peak Ground Accelerations (PGA) (Fukushima and Tanaka, 1990). Empirical relationships between parameters of larger isostatic lengths of macro-seismic intensities and magnitudes have also been used to determine the seismic source (Marín et al., 2008). This methodology provides estimates of seismicity levels, particularly for areas where the history of seismic recurrence is poor or with little information. One of these tectonic areas, which is located in the eastern flank of the Pacific ring of fire is the northwestern coast of Ecuador at the border with the southwestern coast of Colombia. This area is geodynamically characterized by an active subduction zone where the Nazca oceanic plate (with a direction of N80 ° E, and a displacement velocity of 47 mm / yr) collides and subducts the continental segments of the South American and Caribbean plates (Berninghausen, 1962; Barazangi and Isacks 1976; Kanamori and McNally, 1982; De Mets et al., 1990; Nocquet et al., 2016; Trenkamp et al, 2002; Pararas-Carayannis, 2012; Toulkeridis et al., 2017) (Fig. 1).

For the continental territory of Ecuador, it has been possible to establish two main seismic sources, (1) the tectonic zone of the subduction interface, and (2) the crustal (or superficial) geological faults located within the continental segment. The main seismogenic structure, the subduction zone, which is located between 52 and 127 km away from the coastal limits of the province of Esmeraldas, is capable of generating potential earthquakes and subsequent tsunamis in the order of 7.6≤Mw≤9.0 (Fig. 2). The oblique convergence between the subducting Nazca plate with respect to the continental plate, controls in part the development, distribution and kinematics of the crustal faults (ie, Veloza et al., 2012).

In this current study, we evaluated only the crustal faults delineated in the continental segment of the provinces of Esmeraldas and northern Manabí and their extension on the continental shelf (ie, Dumont et al., 2006, Eguez et al., 2002; Michaud, 2012, Michaud et al., 2015, Migeon et al., 2016, Ratzov et al., 2012). These crustal structures have been mapped from field observations, interpretations of geological maps with a scale of 1: 100,000, topography, remote sensing images

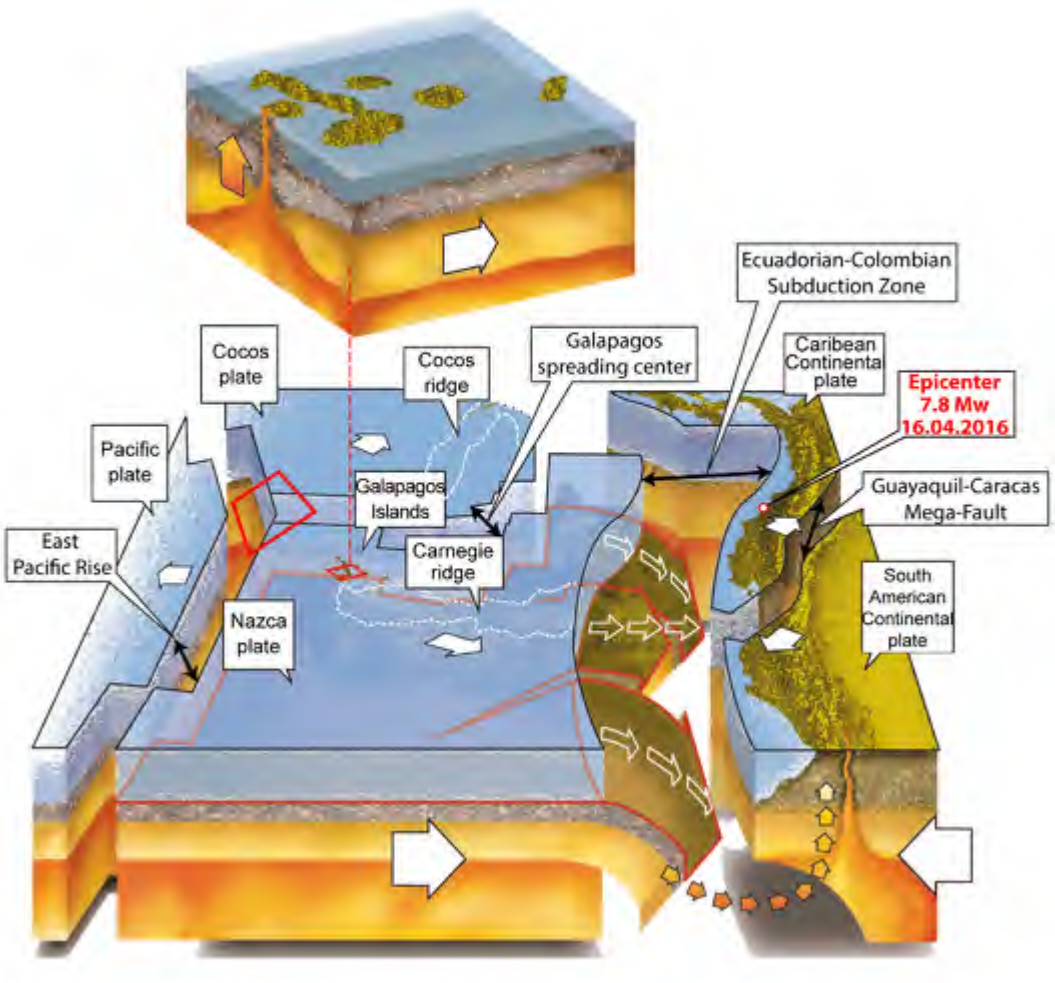

Fig. 1: Geodynamic setting of Ecuador, the Galapagos Islands and the Carnegie Ridge. Adapted from Toulkeridis, 2013 and Rodriguez et al., 2016

and spatial distribution of earthquakes from data available in the catalogs of the Instituto Geofísico of the Escuela Politécnica Nacional in Quito (IG- EPN) and the National Earthquake Information Center of the United States Geological Survey (NEIC-USGS).

The methodological procedure, from a structural geology and coastal geomorphology point of view, has been to delineate the dimensions of the geological fault lengths capable of generating earthquakes and also tsunamis with magnitudes M≥6. Smaller faults that generate earthquakes of 4≤M≤5.5 were not analyzed in this study because of their low probability of causing significant cosmic geological effects on the ground. Records of historical earthquakes associated with geological faults are poorly documented for the coast of Ecuador. However, the recent Pedernales / Muisne earthquake of April 16, 2016 (Mw 7.8) and successive aftershocks due to the seismogenic structure have generated post-seismic effects, such as activation of crustal faults,

which are located between 74 and 115 km distant to the northeast of the epicenter. In the city of Esmeraldas, for the earthquake of Mw 7.8, minor damages of masonry of some houses in the urban center were reported.

Therefore, the main aim of this study has been to apply a methodology to evaluate each capable fault mapped in the territory in order to provide fundamental information of the maximum magnitude and PGA estimates, which may subsequently be applied to determine the level of seismic hazard in densely populated areas or the developing industrial sectors.

2. TECTONICS AND SUBDUCTION EARTHQUAKES OF THE STUDY AREA

Ecuador's subduction zone is approximately 576 kilometers long, but if we consider the subduction geodynamics from the northern coast of Peru reaching the southern Andean being part of the continental territory of Ecuador, then the subduction zone may be as long as 756 kilometers. The subduction interface zone is complex, but may be well distinguished in depth by the variation of the oblique convergence of the subducting Nazca plate towards the continental segment formed by the South American and Caribbean plates (Gutscher et al., 1999: Veloza et al., 2012; Toulkeridis, 2011). Other structural features that may define the areas and borders of seismogenic structures or seismotectonic divisions are the fracture zones of the oceanic crust (Kelleher, 1972; Wiens and Stein, 1983; Carena, 2011).

For the entire coast of Ecuador, three main seismogenic segments may be differentiated along the subduction zone. The first segment being the southern coast, including the Gulf of Guayaquil and the Santa Elena province, the second being the central coast around the Manabí province and the final being the northern coast along the province of Esmeraldas (Chlieh et al., 2014, Chunga, 2010; Chunga and Toulkeridis, 2014; Nocquet et al., 2014, Yepes et al., 2016; Matheus Medina et al., 2016). In the last segment of the seismic structure, the sixth strongest earthquake on the planet occurred on January 31, 1906, with a magnitude of Mw 8.8 (Kanamori and McNally, 1982) has been reported off the coast of Esmeraldas and also in Tumaco located in southwestern Colombia (Pararas-Carayannis, 1980; Ye et al., 2016; Yoshimoto et al., 2017). Later catastrophic earthquakes occurred in the same area in 1958 (Mw 7.6) and 1979 (Mw 7.7; USGS). In the southern zone of Esmeraldas, the delineation of the Galera fracture is well distinguished, so the spatial distributions of aftershock earthquakes of the Pedernales earthquake (2016, Mw 7.8) are culminating in this seismic area (Fig. 2 and 3a, 3b). As previously indicated, the largest documented earthquake for the Ecuadorian-Colombian coastal border occurred on the 31st January 1906 at 10h36 (local time), with a magnitude of 8.8 M_w had with an epicenter in the subduction zone located between 52 and 127 km away from the waterfront. The USGS catalog located the epicenter in the continental segment near the city of Esmeraldas. The tendency of crustal deformation has had a rupture extension of 450 km in length from the line Galera Muisne to Buenaventura, where moderate to high macrosysmic intensities have been documented (Rudolph and Szirtes, 1911). Other studies reported an estimated area of a greater rupture of approximately 500 Km x 180 km (Kelleher, 1972; Kanamori and MacNally, 1982).

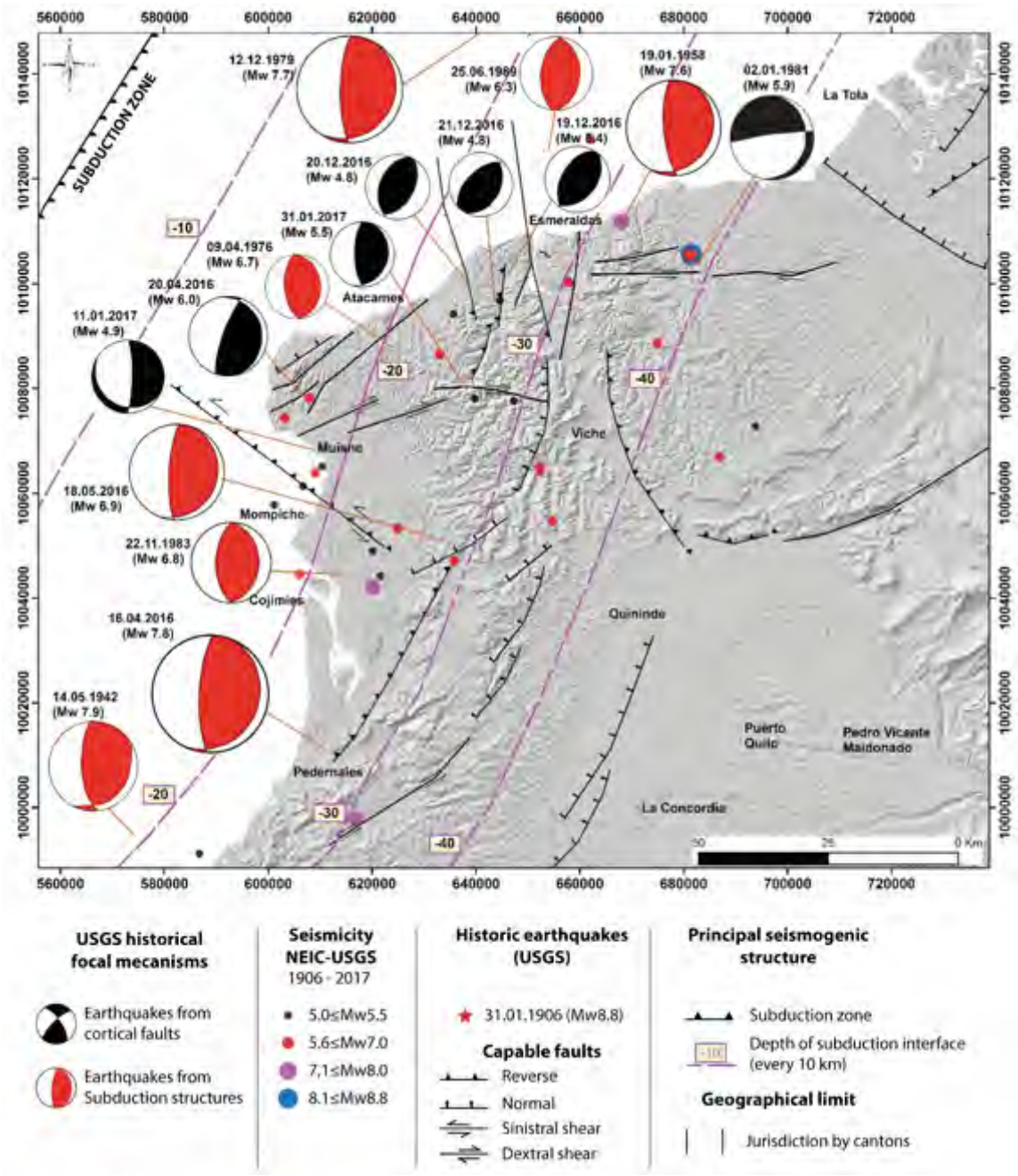

Figure 2. Seismotectonic map of the northern coast of Ecuador. Historical earthquakes with magnitude 5.0≤Mw≤8.8, some represented by focal mechanisms from the NEIC-USGS catalog, classified as earthquakes by subduction and activation of capable faults. Capable faults delineated in this study with abbreviations from FC01 to FC38, from field observations and literature data by Chunga 2010; Dumont et al., 2006; Eguez et al., 2002; Migeon et al., 2016; Ratzov et al., 2012; Reyes and Michaud, 2012. Depth of the subduction interface from Hayes et al., 2012 and Nocquet et al., 2016.

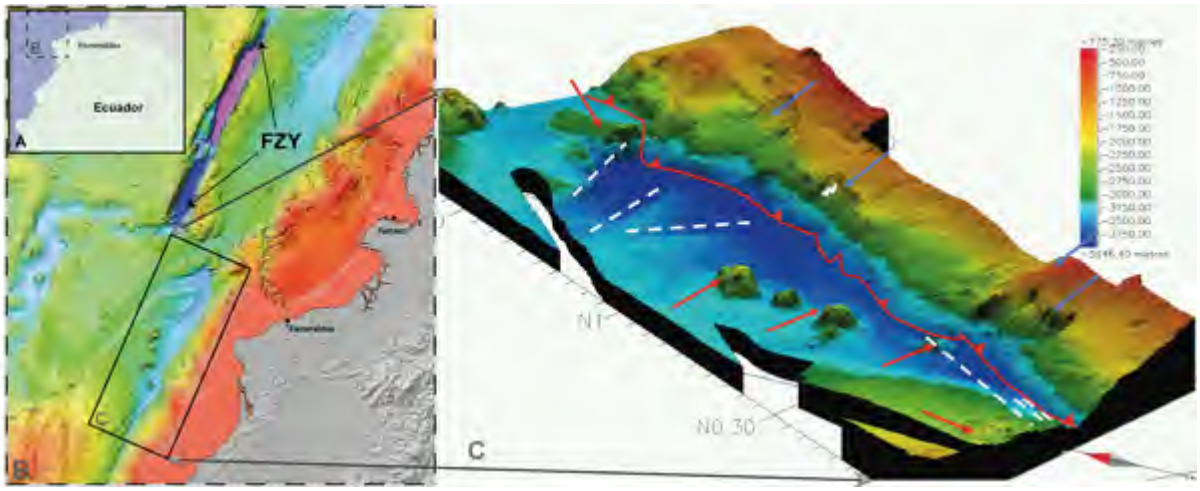

Fig. 3a: Detailed morphology of the continental rim of NW Ecuador, where inlet (b) shows the extension of the Fracture Zone of Yaquina (FZY). Its inlet (c) demonstrates further aspects of Ecuador´s active geodynamics such as deformation front evidencing suture between Nazca Oceanic Plate and Caribbean Continental Plate (red line), some active faults of the oceanic crust at its floor (white dashed lines), Seamounts which enter the subduction zone (red arrows) and some scars of landslides, fissures and submarine debris (blue arrows). Adapted from Collot et al., 2009.

Precursor earthquakes have been documented at 07h00 and 09h00, causing physical and environmental damage in the city of Esmeraldas. These coseismic effects of the second earthquake caused damage to buildings that have been added to the main earthquake (Mw 8.8), where about thirty houses collapsed. For the main event that began at 10:36 am, and lasted between three to five minutes, the premonitory earthquakes allowed many people to look for open spaces, reducing the number of victims. Subsequently, among all the replicas, that of February 2 (4:55 pm) seems to have been the strongest and most extensive, resembling its movement to the main earthquake (Rudolph and Szirtes, 1911).

The coseismic geological effects for the coasts at Esmeraldas, Rio Verde, Limones and La Tola in Ecuador and the sites of Cabo Manglares, Tumaco, Salahonda and Guapi in southwestern Colombia, documented for the epicentral area, primary effects such as subsidence and tectonic intensities of Io VIII to X MSK. The coastal margin from Bahía de Caráquez to Pedernales suff ered modest damages from the earthquake (Io VII MSK). In Manta, the earthquake was already that weak (Io VI MSK), so that many people did not even feel the movement at all (Rudolph and Szirtes, 1911). Impacts of tsunami waves occurred 30 minutes and 50 minutes after the main event, with run-up heights between 5 and 10 meters (Rudolph and Szirtes, 1911). In the site of Tumaco, waves with run-up of 2.5m of height were documented. The city of Esmeraldas was affected by the entrance of tsunami waves through the river and overflowing, flooding of the areas of plains and alluvial terraces (Espinoza, 1992). The location of the epicenter has been referred to the coordinates -79.368344 and 0.954894 at 31 km E of the city of Esmeraldas (USGS, 2017a).

The second record of a strong earthquake and subsequent tsunami for the northern coast of Ecuador occurred on January 19, 1958 with a magnitude of about 7.6 (09h09 TL, local time). The epicenter has been reported 19 km northeast of the city of Esmeraldas with the coordinates -79.4889 and 1.0106 (USGS, 2017b), which by its proximity documented the collapse of 30% of the buildings and the cracking of numerous buildings, 15 dead and 45 wounded (ie, Ramirez, 1958). The duration of this earthquake has been of about 35 to 45 seconds, and the maximum intensities with effect in the field extended up to Tumaco, where no victims were reported. In Cabo Manglares liquefaction has been evidenced of sandy soils with water expulsion to gushes of the open cracks in zone of alluvial plains estuaries. Several primary coseismic effects have been documented, such as a tsunami with a run-up height between 2.0 and 5.9 m (Lockridge, 1985), which devastated part of the coastal towns of Esmeraldas, while in the port of the city four custom guards drawn due to a damaged and sunk boat (ie, Ramirez, 1958). In addition to the earthquake and its primary coseismic effects such as the tsunami, increased intensity and run-up waves may be associated with the re-activation of multiple submarine landslides in the continental slope and in the Esmeraldas canyon (Figure X). The strongest aftershocks were documented on February 1 at 11:20 a.m., 1:10 p.m. and 15:54 p.m., the latter with the highest intensity. Ramírez (1958) documents two earthquakes until April 14, 1958 with epicenters in Esmeraldas Bay, where one person died and 14 were injured.

The third documented earthquake occurred in December 12, 1979 (Mw 7.7, Ms 7.9) at 02:59 local time, with an epicenter in the Pacific Ocean with the coordinates -79.359866 and 1.598427, (Pararas-Carayannis, 1980; USGS, 2017c), located 75 km northeast of the city of Esmeraldas and some 54 km northwest of the village of La Tola. The maximum intensities of VII to IX (IMM) were documented from Tumaco to Bozan, having a length of around 122 km in the southern coastal margin of Colombia. There, the primary coseismic effects of tectonic subsidence determined values between 0.15 m to 0.80 m of vertical displacement, while the site San Juan reached the maximum values of 1.2 to 1.6 m (Herd et al., 1981). An uplift of marine terraces has not been evidenced in the epicentral area.

For the coastal margin of Limones and San Lorenzo there are no field evidences of coseismic effects, but because of its proximity to the Tumaco site, there are certain features of subsidence and side effects attributed to the intensity of about VIII MSK (Herd et al. 1981). Liquefaction phenomena of sandy soils, sinkholes, cracks in the ground, lateral spreading and sand boils were evidenced in Tumaco (Pararas-Carayannis, 1980; Herd et al., 1981). The damages on buildings in the city of Esmeraldas were mild to moderate with an assignment of intensity of about VII, while no victims were reported. Pararas-Carayanis (1980) estimates a structural trend NW and SE of the seismic zone and a propagation of Tsunami waves with greater effect towards the NE, where the coasts of San Juan and El Charco have been washed away by waves with run-up heights between 2 to 5 meters, 6 minutes after the main earthquake. The tide level has been in its lowest position, deducing that the effects might have been more serious even with affectation for the Ecuadorian coasts if the tsunami appeared during the high tide (Espinoza, 1992). Aftershocks of moderate earthquakes that reached the magnitude of Ms 5.9 have been recorded on December 13, December 24 (Ms 5.3), December 31 (Ms 5.5) and January 7, 1980 (Ms 4.6, mb 5.1) (Herd et al. al., 1981).

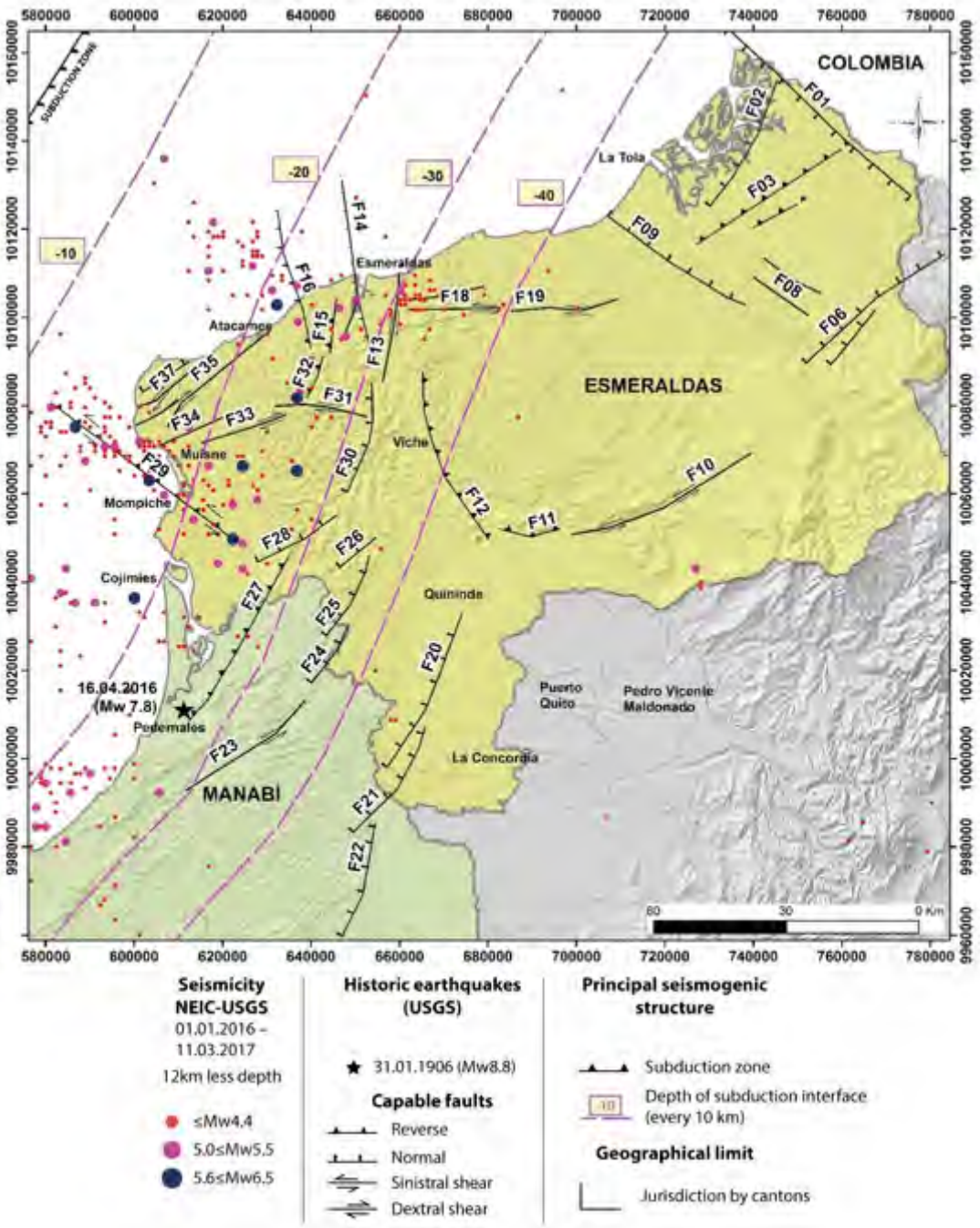

Figure 4. Capable faults and their recent activity from earthquakes recorded at a focal distance of less than 12 km. Earthquakes obtained from the IGEPN, for the time period from January 2016 to March 2017. The interrupted line represents the depth contours of the subduction interface (Hayes et al., 2012, Nocquet et al.). Greater activation of crustal faults is evidenced after the Pedernales earthquake of April 16, 2016 (Mw 7.8). The black star indicates the epicentral position of the recent earthquake of subduction (USGS, 2016; IG-EPN, 2017).

The epicentral area with the highest intensities of the Pedernales earthquake of April 16, 2016 (Mw 7.8, local time 18h58), includes the town of Pedernales and its neighboring communities of Coaque, Jama and Canoa, where the Imax IX - X ESI (Seismic Intensity, Michetti et al., 2007) have been assigned, based on evidence of coastal survey, liquefaction of soils, sinkholes, natural and stabilized slope landslides, cracks in natural soils, surface faults, transverse and longitudinal fractures In asphalt and concrete tracks (Chunga et al., 2017; Toulkeridis et al., 2017).

All of these historical earthquakes on the northern coast of Ecuador have been documented in the NEIC-USGS catalog, which provide seismicity information from 1906 to 2017, reporting 41 earthquakes in the order of magnitudes of $5.0 \leq M \leq 8.8$. Many of these earthquakes have hypocentral distances of less than 20 km in depth, and are attributed to crustal fault systems since the subduction interface zone is deeper (Fig. 4). The IGEPN's national seismological network provides additional information on seismic movements since 1988 (IG-EPN, 2017).

3. DOCUMENTED EARTHQUAKES FROM CAPABLE FAULTS

The recent Pedernales earthquake (Mw 7.8) on April 16, 2016 has provided a large amount of seismological information indicating the re-activation of smaller, capable faults in the continent, particularly in the province of Esmeraldas. In this study, earthquakes with a hypocentral distance of less than 12 km from January 2016 to March 2017 (Fig. 4), with an earthquake projection (IGEPN) and the focal mechanisms (USGS), have been used to classify the structural trend and types of faults capable of generating earthquakes. Hereby, the city of Esmeraldas, have presented a greater seismic activity of at least eight surface faults. These crustal faults have tectonic domain of inverse stress fields with shear components, and others with sinistral and dextral shear or transform faults (Fig. 2 and 4).

The sites from Cojimíes to Muisne have smaller dimensions of coseismic geological effects, where they reached and assigned degree of ESI-07 VIII. In the coastal strip between Cube-Tacu sa and Colope, it has been verified that the unstable natural slopes of clay and silt material that frequently affect the road, did not report rock falls or even minor landslides during the earthquake. In the urban center of the city of Esmeraldas minor damages of masonry of some houses have been documented (Fig. 6a-d). The intensity recorded in this sector of the province of Esmeradas has been of VI ESI-07 (Chunga et al., 2017). Oceanic tsunami propagation with oscillations of ~ 0.5 m / min has been recorded for the city of Esmeraldas between 7:06 p.m. to 7:09 p.m., while the wave amplitude did not reach the highest level since it occurred at low tide (Fig. 1 and 3; Toulkeridis et al., 2017).

In this area, historical earthquakes of moderate magnitude with fault location responsible for the activity are not well documented yet. The oldest well-documented event associated with the activation of a crustal fault is referred to the earthquake of April 9, 1976 (Mw 6.7, depth 9 km). As the city of Esmeraldas has been constructed above clayey and silty sediments within an environment of deposition of a river delta. Therefore, in saturated soils of plains and alluvial terr-

Figure 5. Spatial distribution of geomorphological features for the city of Esmeraldas, with the following abbreviations: Qa, floodplain alluvial plain; Qb: islet of flood barriers; Qt: alluvial terraces; Qc: quaternary colluvial soils; Mb: hills formed by lithologies of the Miocene and Pliocene formations Onzole and Bourbon. Photo City Courtesy: "photo & video drone Esmeraldas". Flood-prone geomorphological features may be considered to estimate the maximum run-up of tsunami waves.

aces, damages were evidences in foundations such as the Delfina Torres de Concha Hospital, the schools “5 de Agosto” and “Juan Montalvo” as well as the Central Market and several more buildings (Figure 7a-d).

Another crustal earthquake occurred on January 2, 1981 (Mw 5.9), where the type of potential shear fault is feasible with the focal mechanism information provided by the USGS (Fig. 2). The earthquake of June 25, 1989 (Mw 6.3) in front of the city of Esmeraldas, caused minor landslides and damages in the urban area (information provided by city dwellers). This available information did not indicate whether this earthquake corresponded to the subduction interface dynamics or the activation of the Esmeraldas crustal fault.

Another recent seismic activity associated with reverse-type surface faulting occurred on December 19, 2016 (Mw 5.4, Ml 5.8, depth 4 to 6 km), with an epicenter at the Tonsupa site in the Atacames area, causing damage to 70 buildings, of which 10 collapsed completely (Figure 8; IG-EPN, 2017; USGS, 2017d) being found on saturated sandy soils of a coastal plain. The next day, another earthquake of 5.2 shook the same coastal area. The last moderate earthquake report of activation of the Atacames fault (referred to as F16) has been on January 31, 2017, at 09:22 local time (Mw 5.5, Ml 5.7, depth 9 km). A particular case is that this earthquake occurred seven

Figure 6a-d. Minor damage in the center of the city of Esmeraldas by the earthquake of Pedernales of April 16, 2016 (Mw 7.8). Upper images from left to right referring to the Bolivar and Manuela Cañizares direction. Bottom images from left to right, referring to the addresses December 6 and Piedrahita, and Ricaurte and / Colon and Eloy Alfaro. Photo courtesy: "photo & video drone Esmeraldas".

minutes after the tsunami simulation organized by the Secretary of Risk Management. Damages occurred on the building of the Municipality of the city of Esmeraldas, with cracking in the masonry and collapses of some smaller walls. For the Atacames site, two buildings were also slightly affected with damage on their walls.This documented information may allow to underestimate in the assessment of seismic risk, because due to the lack of geological and seismological data the north coast may be considered as an area of seismicity generated by surface geological faults of moderate levels. Here the importance of applying this current method that allows to characterize the active or capable faults of generating crustal earthquakes with $6.0 \leq M \leq 7.3$. This would allow to obtain valuable information on the seismic potential of each fault, providing data of maximum magnitudes estimated and the PGA that could generate each geological fault in a certain site of interest.

TABLE 1. Moderate to high earthquakes, documented in the NEIC-USGS catalog, in the order of Mw≥5.0 (USGS, 2017d). The shaded squares represent the earthquakes that originated tsunamis with run-up wave heights between 1 and 5 meters. For the 1906 earthquake, wave heights between 5 and 10 meters have been documented (Rudolph and Szirtes, 1911).

Ref.	Year	Month	Day	Mw	Lat.	Long.	Depth (Km)
1	1906	1	31	8,8	0,955	-79,369	20
2	1942	5	14	7,9	-0,020	-79,950	20
3	1944	10	23	6,7	0,605	-79,320	20
4	1958	1	19	6,8	1,153	-79,543	28
5	1958	1	19	7,6	1,011	-79,489	28
6	1958	2	1	6,3	1,446	-79,146	25
7	1958	2	1	6,3	1,550	-79,305	25
8	1958	2	1	6,9	1,541	-79,338	15
9	1958	4	15	6,1	0,907	-79,581	25
10	1958	4	14	6,8	0,801	-79,428	25
11	1958	4	3	5,7	1,406	-79,547	25
12	1974	3	10	5,6	0,403	-80,047	43
13	1976	4	9	6,7	0,782	-79,804	9
14	1979	3	1	5,6	0,673	-80,073	33
15	1979	12	12	5,0	1,542	-79,377	33
16	1979	12	12	7,7	1,598	-79,358	24
17	1983	11	22	6,6	0,482	-79,877	55
18	1983	12	21	5,2	0,400	-79,907	40
19	1986	1	19	5,0	0,555	-80,041	33
20	1989	6	25	6,3	1,134	-79,616	15
21	1995	7	20	5,0	0,522	-80,091	33
20	1989	6	25	6,3	1,134	-79,616	15
22	1995	10	10	5,1	1,123	-79,350	56
23	2004	6	1	5,4	0,706	-79,744	24
24	2007	12	10	5,1	0,589	-80,007	39
25	2010	11	25	5,4	0,443	-79,920	43
26	2012	2	8	5,2	0,658	-79,258	65
27	2014	6	16	5,7	1,644	-79,250	15
28	2014	3	9	5,6	1,657	-79,350	6
29	2015	5	30	5,3	1,220	-79,570	13
30	2016	12	19	5,4	0,875	-79,700	10
31	2016	12	12	5,2	0,852	-79,780	35
32	2016	7	11	6,3	0,581	-79,630	21
33	2016	7	11	5,9	0,587	-79,630	17
34	2016	5	18	6,9	0,495	-79,610	30
35	2016	5	18	6,7	0,426	-79,780	16
36	2016	4	23	5,7	0,613	-80,250	10
37	2016	4	20	6,0	0,707	-80,030	10
38	2016	4	20	6,2	0,639	-80,210	14
39	2016	4	19	5,6	0,578	-80,020	11
40	2016	4	16	7,8	0,381	-79,920	21
41	2017	1	31	5,5	0,702	-79,676	10

Figure 7a-d. Physical damage caused by the earthquake of 9 April 1976 (Mw 6.7). Upper images from left to right referred to the site of the school "5 de Agosto" and the Central Market. Lower images from left to right, referring to the damages of the "Delfina Torres de Concha" hospital and buildings of the company CEPE - Petroecuador, in the city of Esmeraldas. Photo courtesy: Triconsul.

4. ESTIMATION OF MAXIMUM MAGNITUDES AND PGA FROM THE ANALYSIS OF CAPABLE FAULTS

For a better understanding of the structural geological terminology that we applied in our analysis, we define "capable" fault and potential source of future earthquakes, that structure that evidenced dislocations or superficial displacements during the last 30,000 years (IAEA, 2002), and / or if historical or instrumental seismicity is associated with a particular fault (Chunga, 2010). On the other hand, a fault is considered to be "potentially active" and is considered a potential source of future earthquakes if surface dislocations are evident at least once in the last 50,000 years (IAEA, 2002; Robert and Michetti, 2004; Michetti *et al*., 2007).

With this definition and in order to understand the crustal seismicity levels of the northwestern coast of Ecuador, a catalog of geological faults has been elaborated that includes 38 fault segments capable of deforming the surface of the terrain and generating potential moderate to high earthquakes, in a range of magnitudes from 6.0 to 7.3 degrees (Fig. 7). Earthquakes may be

measured by their magnitude, macro-seismic intensity and PGA. The maximum PGA values estimated in our analysis have been in the order of 0.26g to 0.42g. The database includes mapped faults in the sea floor and part of the continental segment of the provinces of Esmeraldas and Manabí (Table 2). This structural geological information has been obtained from a variety of sources (Dumont et al., 2006; Eguez et al., 2002; Migeon et al., 2016; Ratzov et al., 2012; Reyes and Michaud, 2012), providing relevant information on the geometry and kinematics of each of the geological faults as well as evidence of vertical displacement from late Pleistocene to Holocene.

The geometric parameters for each of the selected faults include: (1) the spatial projection of the fault in the ground, (2) geometry and kinematics of the fault, (3) the structural immersion and estimated angle of displacement of the fault where in focal mechanism analysis it is called rake or direction of the fault and (4) the width of the seismogenic structure. It is fundamental to note here that if a fault has been modeled with several short segments instead of long segments, the maximum magnitude will be lower, and a fault slip rate requires many smaller earthquakes to accommodate a cumulative seismic moment (Well and Coppersmith, 1994).

Figure 8a-d. Structural damage caused by the earthquake of 19 December 2016 (Mw 5.4, hypocenter 4 km). Upper images from left to right refer to the collapse of foundations at the Atacames site. Bottom images from left to right, referring to the site Tonsupa, province of Esmeraldas. Photo courtesy: "photo & video drone Esmeraldas".

Estimated Magnitude (Mw) = 5.08+1.16*LOG (Lf)
Displacement of fault (in meters) = EXP(-1.38+1.02*LOG(Lf)
Where Lf, expresses the length of the capable fault.
Later, modifications and corrections have been proposed to the previous formula to estimate maximum magnitudes (Leonard, 2010).
Mw = a*log (Lf)+b; being the coefficients of, a=1.52 y b=4.33
Estimated Magnitude (Me) = 1,52*LOG (Lf)+4,33

The most common approach to estimate the maximum magnitude is through a comparison of the fault rupture length and its associated magnitude. Confirming the aforementioned, we estimated the maximum magnitudes for each of the individualized crustal faults in this study and the maximum vertical displacement based on empirical magnitude-earthquake-rupture / geological fault displacement empirical relationships proposed by Well and Coppersmith (1994).

A new proposal includes the earthquake scale ratio for each type of capable fault (Wesnousky, 2008), such as:
Transform (shear) faults; Mw = 5.56+0.87*Log(Lf)
Normal faults; Mw = 6.12+0.47*Log(Lf)
Reverse faults; Mw = 4.11 +1.88*Log (Lf)

These regression equations indicate that not all types of faults of the same dimension are able to generate earthquakes of the same value of magnitude (Stirling et al., 2013; Wesnousky, 2008). This theory has been applied for the delineated faults In the northwestern coast of Ecuador, where it is defined that those faults of the reverse type have been considered potentially capable of generating earthquakes larger than those of equal length than those of shear and normal types (Fig. 9).

Another determination of earthquakes is the PGA, of which the equation proposed by Fukushima and Tanaka (1990) has been applied. These values of PGA may be compared with the seismic zonation map of Ecuador, of the Ecuadorian Construction Standard (NEC, 2015).

The equation applied in this study has been:

Estimated PGA = (10^(0,41*Me-LOG10(Hf+0,032*10^(0,41*Me))-0,0034*Hf+1,3))/980

Hf, is the hypocenter or depth in kilometers of the geological fault.

With all these obtained data, estimations of magnitudes and PGA have been represented with spatially models of surfaces and contours associated to the active tectonics of the territory (Fig. 10), while programs or software's platform GIS and Surfer have allowed to interpolate and transform values of XYZ (X: coordinate latitude, Y: coordinate length, Z: value of magnitude), applying the gridding and nearest neighbor method on isovalues maps, as illustrated in figure 7 for data interpolations Mw and their tectonic confrontation with capable faults. The reliability levels for each of the capable faults have been applied, from seismic analysis (records of

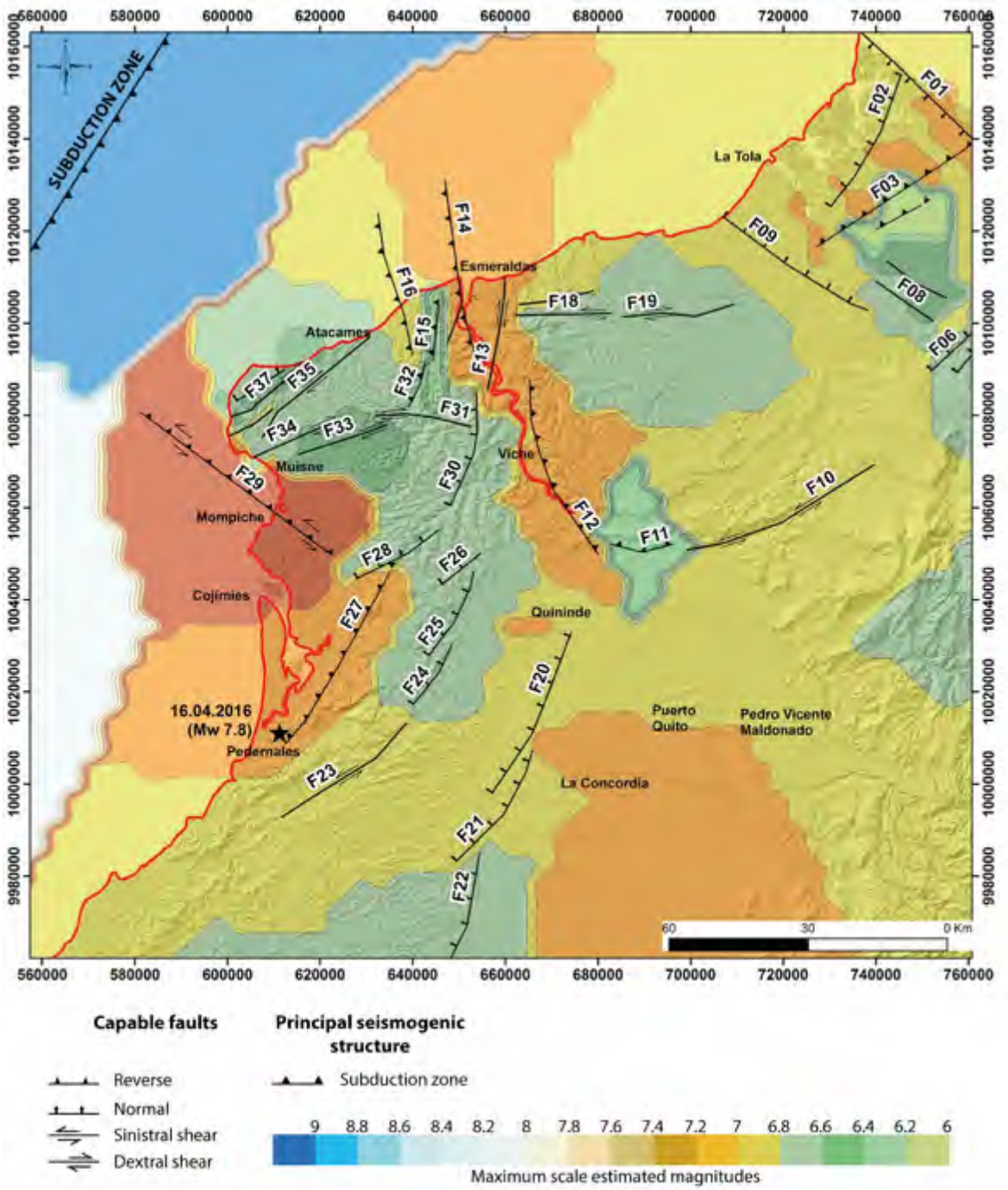

Figure 9. Estimation of maximum possible magnitudes obtained from fault analysis using the method of equations proposed by Wesnousky (2008). The abbreviations F-01 to F-38 indicate the numbering of the geological faults delineated in the north coast of Ecuador. Crustal faults have been delineated from Chunga 2010; Dumont et al., 2006; Eguez et al., 2002; Migeon et al., 2016; Ratzov et al., 2012; Reyes and Michaud, 2012.

instrumental earthquakes delineated along the structure) and morphological (faults escarpments or delineation of reliefs associated with tectonic collapse or sinking), classifying them in three categories: * I (true), ** II (deductible), and *** III (uncertain or hypothetical) (see Table 2). For a "true" structural reliability level, it is necessary that geological faults present evidence of seismicity and lateral displacements in the terrain during the Holocene. For a "deduced" level the fault must have displacement or dislocation of the well distinguished terrain in the morphometry of the relief, while for a "hypothetical" level it is when the structural guidelines may be associated with an active fault but the direction of the displacement remains unknown, or also when the earthquakes are aligned with depth less than 10 km.

The 41 capable faults selected in this study are able to generate earthquakes in the order of magnitudes ranging from 6.0 to 7.3, with the exception of the northern segment of the subduction zone located 53 and 121 km away from the coast of the province of Esmeraldas, which would be able to generate a potential earthquake in the order of 9.0 degrees of magnitude and PGA $\geq$ 0.50 g. The FC14 fault of reverse type with sinistral shear component is the closest to the city of Esmeraldas. In fact, the most developed urban area is in the area of a hanging wall. This fault is able to generate earthquakes in the order of M 7.18 and PGA in rock of 0.41g. Other faults of similar magnitudes are referred to FC03, FC12 and FC27. The Galera fault FC29 may reach the maximum of M7.33 and a PGA of 0.42, calculated from the application of Wesnousky (2008). The distance between the city of Esmeraldas and these potential faults are in the order of 25 to 77 km. However, faults of smaller magnitudes $6.1 \leq M \leq 6.9$ are located less than 10 km from the city of Esmeraldas, which are also considered because of their proximity and potential damage to the urban area, yielding a PGA between 0.27 g and 0.38 g (Fig. 10).

The information of moderate and strong earthquakes whose origin is associated to crustal geological faults, are little documented for the province of Esmeraldas. Crustal earthquakes from capable failures are reported for April 9, 1976 (Mw 6.7), January 2, 1981 (Mw 5.9), and June 25, 1989 (Mw 6.3), the latter may be associated with the Esmeraldas fault (FC14). For the Atacames fault (FC16), recent earthquakes had higher activity records from December 2016 to January 2017, reaching a Mw 5.5 (USGS, 2017d). In the area of Galera, an earthquake of Mw 6.0 occurred on April 20, 2016, considered an aftershock because it is located in the epicentral area of the earthquake of Mw 7.8, however its association with the activation of the FC35 fault is not ruled out.

1. THE ESMERALDAS FAULT AND THE SEISMIC RISK OF THE CITY OF ESMERALDAS

Remote sensing images, digital terrain models and bathymetry, earthquake focal mechanisms and gravimetric data have allowed us to characterize the dynamics and geometry of the Esmeraldas fault, which is abbreviated as F14 (Table 2) in the fault catalog. From a point of view of the gravimetric analysis for the province of Esmeraldas, we proceed from a data grid with a spacing of 1 minute (~ 2 km) between each measurement (Smith and Sandwell, 1997; Sandwell and Smith, 2009; Sandwell et al., 2013; Sandwell et al., 2014).

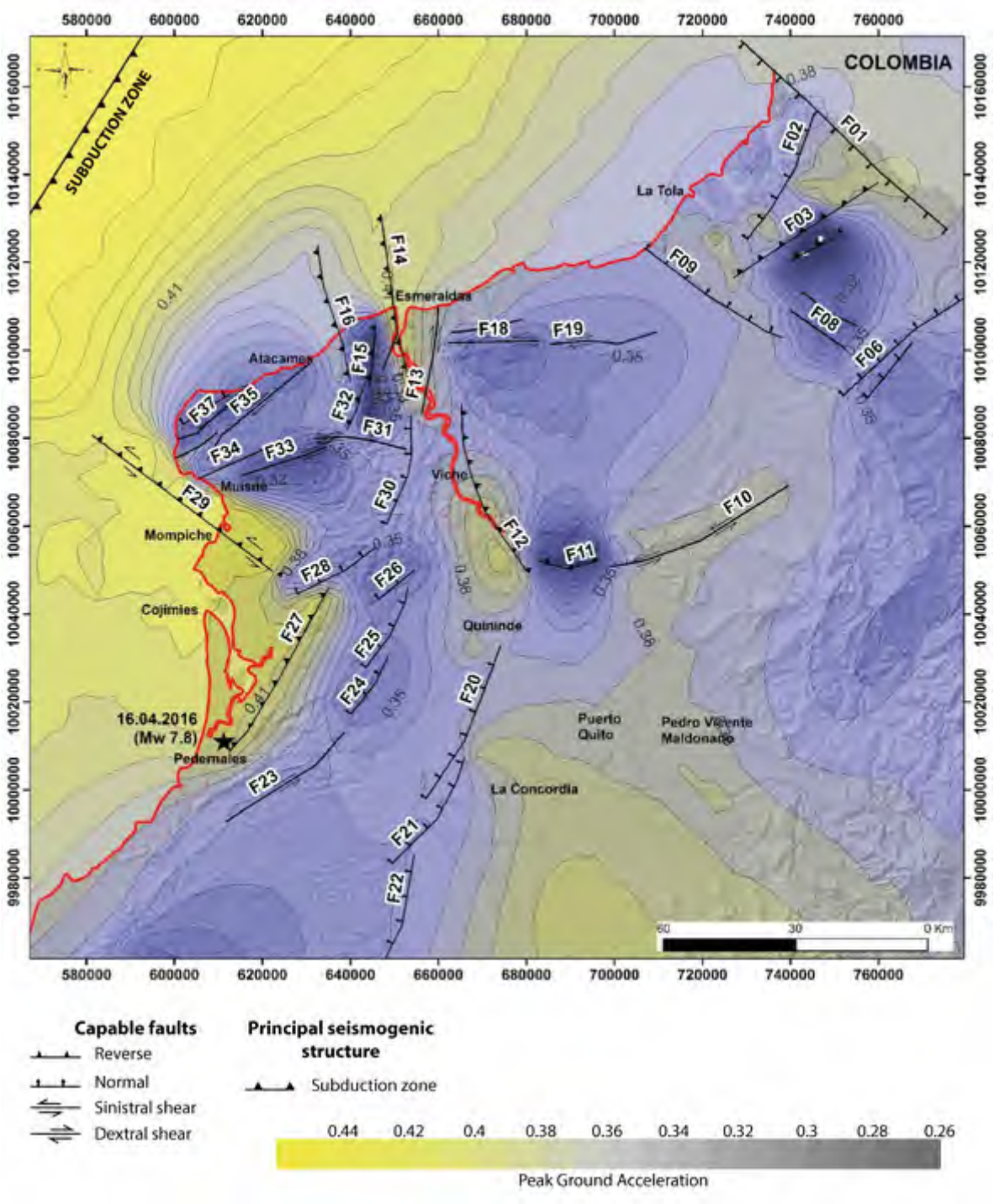

Figure 10. Estimation of obtained PGA from fault analysis using the method of equations proposed by Fukushima & Tanaka (1990). The abbreviations F-01 to F-38 indicate the numbering of the geological faults delineated in the north coast of Ecuador (Table 2).

The gravimetric data are based on the EGM2008 terrestrial gravimetric model, which was published by the National Geospatial and Intelligence Agency of the United States (NGA, 2013). This model has been calculated from combined models, that is, a robust estimation based on gravimetric measurements, terrestrial, marine and satellite models, which were tuned by spherical harmonic algorithms of degree and order of 2159, containing also additional coefficients of degree 2190 and order 2159. The gravimetric anomaly map of the Esmeraldas region and in particular for the urban area corresponds to a vertical derivative (Z), which has been processed by the software Geosoft Oasis Montaj 6.4 for the calculation of the topographic correction using a radius Minimum correction up to 500 meters, and a Bouguer correction with a reduction density of 2.7 gr / cm^3 (Fig. 11).

This first analysis plus the geomorphological features and details of bathymetric dips of the Esmeraldas canyon have allowed to delineate the length of 43 km of the fault with a structural tendency of 262/40 (dip-direction / dip). The review of focal mechanisms of surface earthquakes provided by the USGS, allowed to know the tectonic environment of deformation, being sinistral shear. Afterwards, regression equations applied to the geometric and kinematic parameters of faults allowed the estimation of the maximum magnitudes (Leonard, 2010; Stirling et al., 2013; Wells and Coppersmith, 1994; Wesnousky, 2008). For the Esmeraldas fault, this application estimates a maximum magnitude of 7.1. Hypocentral distances of crustal earthquakes near the fault allowed to associate the depth of a fault plane between 9 to 12 km (Table 3).

One of the most notable displacement features of the fault may be observed in the 1: 100,000 geological map where the upper Onzole Formation (Pliocene age) has a shear displacement in the order of 800 to 1500 m, and the formation Angostura (Mid-Miocene) in the order of 2.4 km. The Esmeraldas fault cuts off all this rocky stratigraphic sequence from the Miocene - Pliocene, so that an active tectonic rupture activity has been deduced since the Pleistocene.

From the point of view of the structural geological analysis of the Esmeraldas fault, considering the relation of moderate seismic activity with the well preserved geomorphological evidence, and the displacement rupture initiated in the Quaternary, we propose a rate of 0.4 to 0.8 mm / year for the Esmeraldas fault (Table 3). These values are confrontable with geomorphological features related to the fault activity proposed by Slemmons and Depolo (1984).

Geotechnical and superficial seismic information in the city of Esmeraldas, and geological sections, have evidenced a deformation of recent sediments as a consequence of the compressional effort exerted to the hanging block where the urban area has developed. The zone of greater deformation would occur it in the northern part of the city, and the depth of the interface rock / sediment in this place is closer to the surface, with folded layers which may be well delineated from radargrams (Chunga, 2017).

The seismic hazard levels increase in the city of Esmeraldas, due to the proximity of the geological fault capable of generating earthquakes in the order of M 7.1. In addition, the developed urban area is situated above the hangingwall position of the fault.

TABLE 2. Catalog of capable faults of generating earthquakes greater than 6 degrees of magnitudes. Estimations of maximum magnitudes for faults from applications of regression equations proposed by (^) Wesnousky (2008), and other formulas proposed by (*) Well & Coppermisth (1994) and Leonard (2010). PGA calculations are based on Fukushima & Tanaka (1990)

Capable Fault	Type	Length (km)	Depth (km)	Dist. to city (km)	Azim.	Rake	Width (km)	Structural position	Maxim. displac. (m)*	Estim. Magnit. from type of fault^	Reliability levels	PGA in Rock	Hypo-central distance (in km)	Refer.
F01	Normal	63	12	101	134	-90	11	Hanging wall	1,6	6,97	deducted	0,38	101,71	Dumont et al., 2006
F02	Normal	32	12	81	28	-90	9	Hanging wall	1,2	6,83	deducted	0,36	81,88	Dumont et al., 2006
F03	Reverse	39	12	77	58	90	10	Hanging wall	1,3	7,10	true	0,40	77,93	Dumont et al., 2006
F04	Reverse	11	12	90	60	90	7	Hanging wall	0,7	6,07	deducted	0,26	90,80	Dumont et al., 2006
F05	Sinistral shear	15	12	92	118	5	8	left-lateral	0,8	6,47	true	0,32	92,78	Dumont et al., 2006
F06	Normal	40	12	103	52	-90	10	Hanging wall	1,3	6,87	deducted	0,37	103,70	Dumont et al., 2006
F07	Normal	16	12	108	32	-90	8	Hanging wall	0,9	6,69	deducted	0,34	108,66	Dumont et al., 2006
F08	Dextral shear	15	12	89	122	-175	8	right-lateral	0,8	6,61	true	0,33	89,81	Dumont et al., 2006
F09	Normal	37	12	58	123	-90	10	Foot wall	1,2	6,86	deducted	0,37	59,23	Dumont et al., 2006
F10	Dextral shear	44	12	75	66	-175	10	right-lateral	1,3	6,92	deducted	0,38	75,95	Michaud, 2015
F11	Reverse	14	12	64	81	90	7	Hanging wall	0,8	6,26	true	0,29	65,12	Eguez et al., 2003
F12	Reverse	42	12	25	146	90	10	Foot wall	1,3	7,16	deducted	0,40	27,73	Eguez et al., 2003
F13	Dextral shear	25	12	10	12	-175	9	right-lateral	1,0	6,97	deducted	0,38	15,62	Eguez et al., 2003
F14	Reverse	43	12	1	352	90	10	Hanging wall	1,3	7,18	deducted	0,41	12,04	Eguez et al., 2003
F15	Reverse	12	12	6	8	90	7	Foot wall	0,8	6,16	deducted	0,27	13,42	This study
F16	Reverse	32	12	14	348	90	9	Foot wall	1,2	6,94	deducted	0,38	18,44	Dumont et al., 2006
F17	Dextral shear	16	12	13	77	-175	8	right-lateral	0,9	6,87	true	0,37	17,69	This study
F18	Sinistral shear	21	12	13	89	-5	8	left-lateral	1,0	6,61	true	0,33	17,69	Pontoise, 2004
F19	Dextral shear	24	12	36	81	-175	9	right-lateral	1,0	6,70	deducted	0,35	37,95	Pontoise, 2004

Continuation of Table 2

Capable Fault	Type	Length (km)	Depth (km)	Dist. to city (km)	Azim.	Rake	Width (km)	Structural position	Maxim. displac. (m)*	Estim. Magnit. from type of fault^	Reliability levels	PGA in Rock	Hypo-central distance (in km)	Refer.
F20	Normal	39	12	78	22	-90	10	Hanging wall	1,3	6,87	deducted	0,37	78,92	Eguez et al., 2003
F21	Normal	30	12	103	20	-90	9	Hanging wall	1,1	6,81	deducted	0,36	103,70	Eguez et al., 2003
F21	Normal	30	12	103	20	-90	9	Hanging wall	1,1	6,81	deducted	0,36	103,70	Eguez et al., 2003
F21	Normal	30	12	103	20	-90	9	Hanging wall	1,1	6,81	deducted	0,36	103,70	Eguez et al., 2003
F22	Normal	27	12	125	10	-90	9	Hanging wall	1,1	6,79	true	0,36	125,57	Eguez et al., 2003
F23	Sinistral shear	34	12	94	51	-5	10	left-lateral	1,2	6,81	true	0,36	94,76	Eguez et al., 2003
F24	Normal	16	12	77	22	-90	8	Hanging wall	0,9	6,69	true	0,34	77,93	Eguez et al., 2003
F25	Normal	21	12	64	3	-90	8	Hanging wall	1,0	6,74	deducted	0,35	65,12	Eguez et al., 2003
F26	Normal	11	12	58	52	-90	7	Hanging wall	0,7	6,60	true	0,33	59,23	Eguez et al., 2003
F27	Reverse	44	12	65	32	90	10	Hanging wall	1,3	7,19	deducted	0,41	66,10	Eguez et al., 2003
F28	Normal	21	12	52	61	-90	8	Hanging wall	1,0	6,74	true	0,35	53,37	Eguez et al., 2003
F29	Reverse	52	12	62	129	90	11	Hanging wall	1,4	7,33	deducted	0,42	63,15	This study
F30	Normal	26	12	22	11	-90	9	Hanging wall	1,1	6,78	true	0,36	25,06	Eguez et al., 2003
F31	Dextral shear	21	12	28	97	-175	8	right-lateral	1,0	6,79	true	0,36	30,46	This study
F32	Reverse	10	12	18	12	-175	7	Foot wall	0,7	6,71	deducted	0,35	21,63	This study
F33	Dextral shear	20	12	34	71	-175	8	right-lateral	0,9	6,44	deducted	0,31	36,06	Michaud, 2015
F34	Dextral shear	17	12	42	66	-175	8	right-lateral	0,9	6,69	deducted	0,35	43,68	Michaud, 2015
F35	Dextral shear	32	12	23	52	-175	9	right-lateral	1,2	6,63	true	0,34	25,94	Michaud, 2015
F36	Dextral shear	11	12	49	52	-175	7	right-lateral	0,7	6,87	deducted	0,37	50,45	Michaud, 2015
F37	Dextral shear	19	12	38	53	-175	8	right-lateral	0,9	6,46	deducted	0,31	39,85	Michaud, 2015
F38	Normal	13	12	42	56	-90	7	Foot wall	0,8	6,64	true	0,34	43,68	Michaud, 2015
ZS	Reverse	400	25	82	32	90	20	Hanging wall	3,6	9,00	true	≥0,50	85,73	Eguez et al., 2003

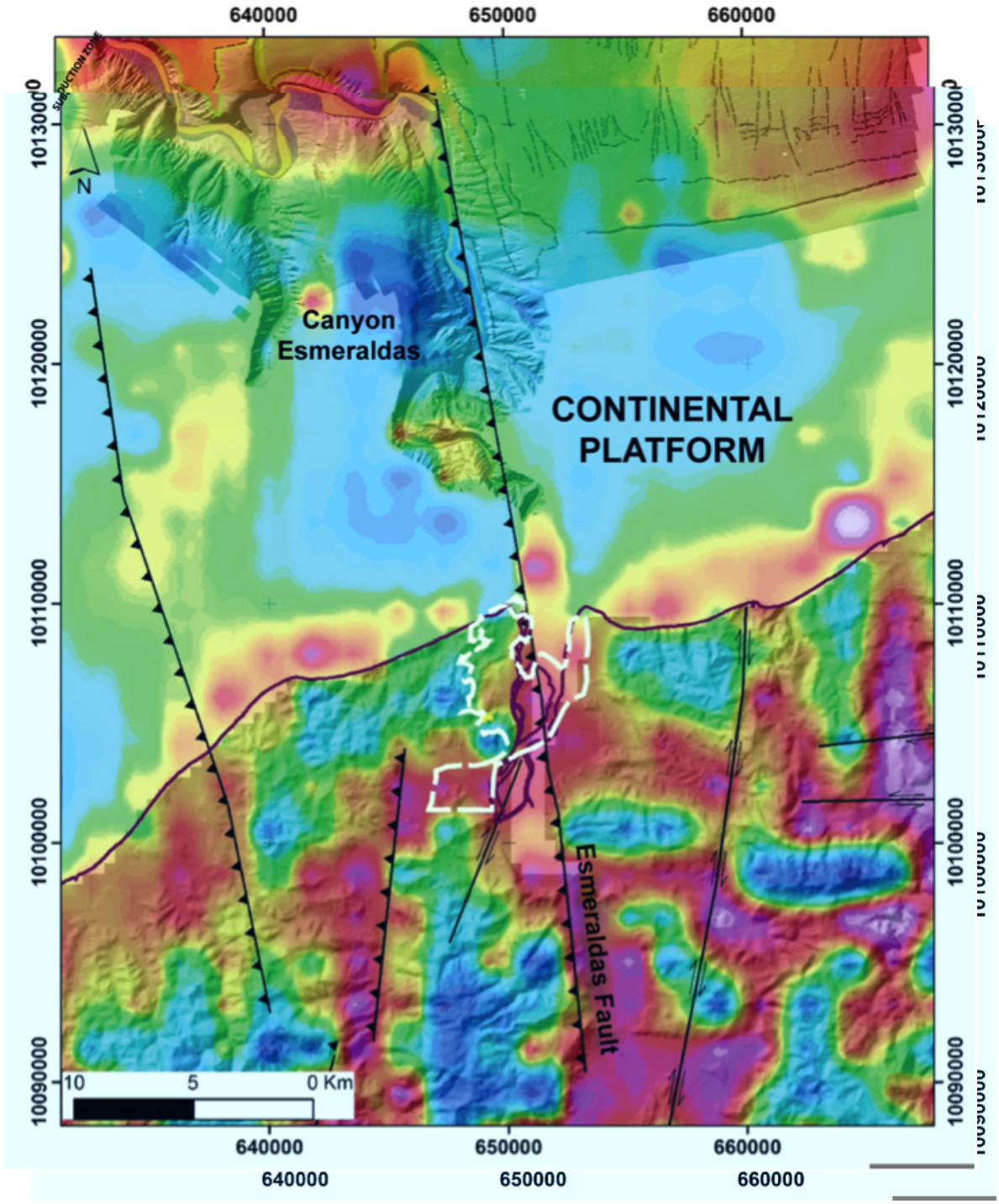

Figure 11. Delineation of the Esmeraldas fault from digital terrain models, gravimetric and seismological data. The interrupted white line is the delimitation of the study area of the city of Esmeraldas.

Table 3. Characterization of the Esmeraldas fault and its kinematic and geometric parameters.

	Seismogenic structure	**Type**	**Estimated length of fault based on morphologic analysis (km)**	**Distance Fault - City (km)**	**Structural fault data (dip-direction/dip)**
Characterization of seismic source for the city of Esmeraldas	Esmeraldas Fault (F-14)	Reverse with sinistral shear component	43	-1	262/40
	Estimated magnitude	**Reliability levels from seismological and morphological analysis**	**Historic earthquakes associated with the fault**	**Position of the city in respect to the fault**	**Displacement rate (mm / year) from geomorphological**
	7,18	true (I) to deducted (II)	09.04.1976 (Mw 6,7) 25.06.1976 (Mw 6,3)	Hangingwall	0,4 - 0,8

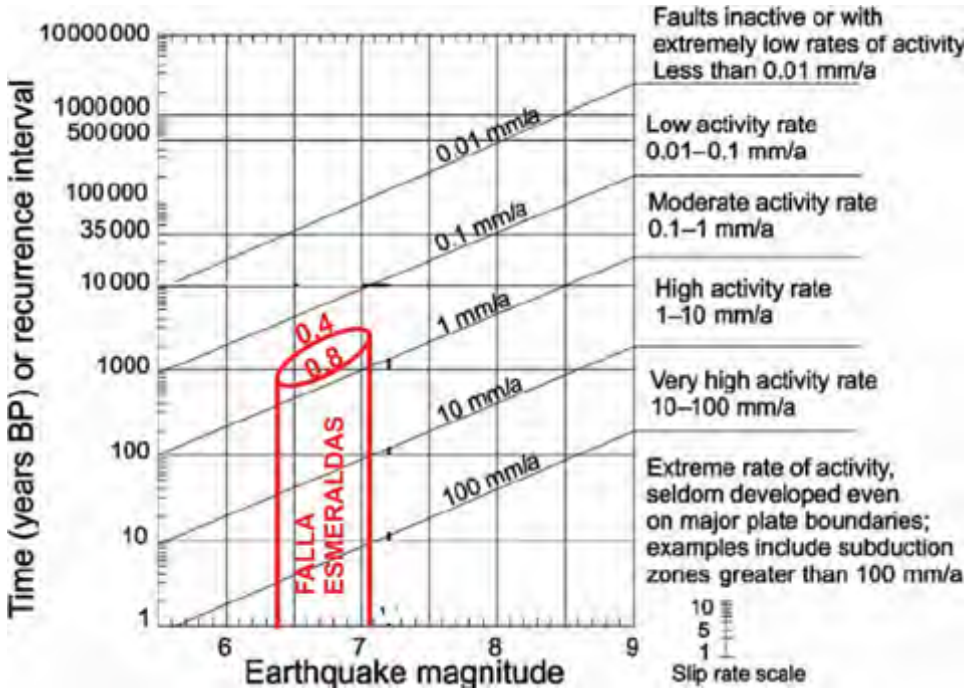

Figure 12. Estimation of the displacement rate of the Esmeraldas fault and its relation with recurrence intervals. Earthquake magnitude reference and recurrence time from Slemmons and Depolo (1984).

Therefore, the estimation of a crustal earthquake from a capable fault with M≥8 is discarded for the northwestern coast of Ecuador. The erroneous calculation to estimate this exaggerated magnitude derives from an oversized geological fault, without considering important parameters such as (a) behavior of kinematics and efforts with variable tendencies, besides the (b) morpho-

logic-structural guidelines that are those that define in the potential segments of seismogenic structures (Chunga, 2010). These two parameters (a and b) have been respected and considered in the present study.

5. CONCLUSIONS

Well documented historical earthquakes for the northwestern coast of Ecuador begin in 1906 with Mw 8.8 and continue in 1958 (Mw 7.6), 1979 (Mw 7.7) until 2016 (Mw 7.8) and are considered to be associated with the dynamic interface of the subduction zone in front of the coasts of the province of Esmeraldas. In all these years, 41 earthquakes have been recorded among subduction and from capable faults, with magnitudes in the order of $5.0 \leq M \leq 8.8$. Crustal earthquakes from capable failures are reported for 1976 (Mw 6.7), 1981 (Mw 5.9) and 1989 (Mw 6.3).

Coseismic effects on the ground may be driven from moderate earthquakes from capable faults and also from strong distant earthquakes such as those from subduction. Coastal urban development in the city of Esmeraldas and communities increases the level of seismic risk by being above sandy saturated sediments and liquefiable sandy silts and clays. Tsunami risk should be considered between 13 and 18 m.a.s.l., which would be able to flood through tsunami run-up waves in the plains and the first alluvial terrace in the city of Esmeraldas. A preliminary paleoseismologic analysis by the authors allows to distinguish deposits of tsunamis of up to 800 m of distance from the coastline assuming the floodplain.

The estimation of a crustal earthquake (and tsunami) from a capable fault with $M \geq 8$ is discarded for the northwestern coast of Ecuador due to the evaluation of parameters such as behavior of kinematics and the consideration of morphologic-structural guidelines that define potential segments of seismogenic structures.

6. REFERENCES

Barazangi M. and Isacks, B.L. (1976). Spatial distribution of earthquakes and subduction of the Nazca plate beneath South America: Geology, v. 4, p. 686-692.

Berninghausen, W.H., 1962. Tsunamis reported from the west coast of South America 1562-1960. Bull. of the Seismological Soc. of America, 52 (4): 915-921.

Carena, S. (2011) - Subducting-plate topography and nucleation of great and giant earthquakes along the South America trench. Seismol. Res. Lett., 82 (5) 629-637, doi:10.1785/gssrl.82.5.629.

Chlieh M., Mothes P.A., Nocquet J.-M., Jarrin P., Charvis P., Cisneros D., Font Y., Collot J.-Y., Villegas-Lanza J.-C., Rolandone F., Vallée M., Regnier M., Segovia M., Martin X., Yepes H. (2014). Distribution of discrete seismic asperities and aseismic slip along the Ecuadorian megathrust. Earth Planet. Sci. Lett. 400, 292_301.

Chunga K. (2010). Shallow crustal earthquakes and seismic zonation for Ecuador through the integration of geological, seismological and morphostructural data (in Italian). University of Insubria. Ph.D. Thesis, p. 165.

Chunga K., Michetti AM., Mulas M., Besenzon D., Ferrario MF., Garces D., Ochoa F. (2017). Intensidad Macrosísmica ESI-07 y Efectos Geológicos del Terremoto de Pedernales del 16.04.2016 (Mw 7.8). VIII Jornadas en Ciencias de la Tierra. Quito, 8/14 de mayo, 207-211.

Chunga, K. and Toulkeridis, T. (2014). First evidence of paleo-tsunami deposits of a major historic event in Ecuador. Science of Tsunami Hazards. 33: 55-69.

Collot J. Y., Michaud F., Alvarado A., Marcaillou B., Sosson M., Ratzov G., Pazmino A., 2009. Visión general de la morfología submarina del margen convergente de Ecuador-Sur de Colombia: Implicaciones sobre la transferencia de masa y la edad de la subducción de la Cordillera de Carnegie. En: Geología y Geofísica Marina y Terrestre del Ecuador desde la Costa Continental hasta las Islas Galápagos. Editores: Collot J. Y., Sallares V., Pazmiño N. Impreso: Argudo & Asociados, Guayaquil-Ecuador. pp. 47-74. ISBN-978-9978-92-737-3.

De Mets, C., Gordon, R.G., Argus, D.F., y Stein, S. (1990). Current plate motions, Geophys. J. Int., 101, 425-478.

Dumont J.F., Santana, E., Valdez F., Tihay J.P., Usselmann P., Iturralde D., Navarrete E. (2006). Fan beheading and drainage diversion as evidence of a 3200-2800 BP earthquake event in the Esmeraldas-Tumaco seismic zone: A case study for the effects of great subduction earthquakes. Geomorphology 74, 100– 123. doi:10.1016/j.geomorph.2005.07.011

Eguez A., Alvarado, A., Yepes, H., Machette, M.N., Costa, C.H., Dart, R.L., and Bradley, L.-A. (2003). Database and map of Quaternary faults and folds of Ecuador and its offshore regions: U.S. Geological Survey Open-File Report 03-289.

Espinoza J. (1992). Terremotos Tsunamigénicos en el Ecuador. Acta Oceanográfica del Pacífico, 7(1), 21-28.

Fukushima Y. and Tanaka T. (1990). A New Attenuation Relation for Peak Horizontal Acceleration of Strong Earthquake Ground Motion in Japan, Bull.Seism.Soc. Am., Vol. 80, No. 4, 757-783.

Gutscher, M.A., Malavieille, J.S.L. and Collot, J.-Y., 1999: Tectonic segmentation of the North Andean margin: impact of the Carnegie ridge collision. Earth Planet. Sci. Lett. 168: 255–270.

Hayes, G.P., Wald, D.J., Johnson, R.L. (2012). Slab1.0: a three-dimensional model of global subduction zone geometries. J. Geophys. Res. Solid Earth 117, B01302 (2012).

Herd DG, Youd TL, Meyer H, C JL, Person WJ, Mendoza C. (1981). The great tumaco, Colombia earthquake of 12 december 1979. Science 211(4481):441-5. doi: 10.1126/science.211.4481.441

http://www.igepn.edu.ec/eq20160416-home

https://earthquake.usgs.gov/earthquakes/search/

IAEA International Agency of Atomic Energy Safety Standards Series (2002). Evaluation of Seismic Hazards for Nuclear Power Plants. Safety Guide. No. NS-G-3.3. International Atomic Energy Agency.

IGEPN (Instituto Geofísico de la Escuela Politécnica Nacional), 2017. Informes de los últimos sismos. (http://www.igepn.edu.ec/portal/ultimo-sismo/informe-ultimo-sismo.html)

Kanamori, H. and McNally, K. (1982). Variable rupture mode of the suduction zone along the Ecuador-Colombia coast. Bull. Seismol. Soc. Am. 72, 1241_1253.

Kanamori, H. and McNally, K.C., 1982. Variable rupture mode of the subduction zone along the Ecuador-Colombia coast. Bulletin of the Seismological Society of America, 72(4), pp.1241-1253.

Kelleher, J. (1972). Rupture zones of large South Amercan earthquakes and some predictions. Journal of Geophysical Research, vol 77, No. 11, pp. 2087-2103.

Leonard M., (2010), "Earthquake fault scaling: Self consistent relating of rupture length width, average displacement, and moment release", Bulletin of the Seismological Society of America, 100 (SA), 1971-1988p.

Lockridge, P. (1985). Tsunamis in Peru-Chile (Report SE-39, World Data Center A for Solid Earth Geophysics, 1985).

Marín J.P., Salcedo E., Castillo H. (2008). Relaciones empíricas entre parámetros instrumentales y macrosísmicos de algunos terremotos fuertes de Colombia. Boletín de Geología. Vol. 30, No. 1, 99-111p.

Medina, A. S. M., D'Howitt, M. C., Almeida, O. P., Toulkeridis, T., and Haro, A. G. (2016). Enhanced vertical evacuation application with geomatic tolos for tsunamis in Salinas, Ecuador. *Science of Tsunami Hazards*, *35*(3): 189-213.

Michaud F., Proust J. N., Collot J.Y., Lebrun J. F., Witt C., Ratzov G., Pouderoux H., Martillo C., Hernandez M. J., Loayza G., Penafiel L., Schenini Laure, Dano A., Gonzalez M., Barba D., De Min L., Ponce G., Urresta A., Calderon M. (2015). Quaternary sedimentation and active faulting along the Ecuadorian shelf: preliminary results of the ATACAMES Cruise (2012). Marine Geophysical Research, 36 (1), 81-98. ISSN 0025-3235

Michetti A.M., Esposito E., Guerrieri L., Porfido S., Serva L., Tatevossian R., Vittori E., Audemard F., Azuma T., Clague J., Comerci V., Gürpinar A., McCalpin J., Mohammadioun B., Mörner N.A., Ota Y. e Rogozhin E. (2007). Intensity Scale ESI 2007. La Scala di Intensità ESI 2007, ed. L. Guerrieri e E. Vittori (Memorie Descrittive della Carta Geologica d'Italia, vol.74, Servizio Geologico d'Italia – Dipartimento Difesa del Suolo, APAT), Roma, http://www.apat.gov.it/site/it-IT/Progetti/-INQUA_Scale/.

Migeon, S., Garibaldi, C., Ratzov, G., Schmidt, S., Collot, J.-Y., Zaragosi, S., Texier, L., (2016). Earthquake-triggered deposits in the subduction trench of the North Ecuador/South Colombia margin and their implication for paleoseismology, Marine Geology (2016), doi: 10.1016/j.margeo.2016.09.008

NEC-15 (2015). Norma Ecuatoriana de la Construcción, Ministerio de Desarrollo Urbano y Vivienda, MIDUVI, Quito.

NGA (National Geospatial and Intelligence Agency of the United States), 2013. EGM2008 – WGS 84 Version. http://earth-info.nga.mil/GandG/wgs84/gravitymod/egm2008/egm08_wgs84.html

Nocquet J.-M., Jarrin P., Vallée M. et al. (2016). Supercycle at the Ecuadorian subduction zone revealed after the 2016 Pedernales earthquake. Nature Geoscience 10, 145-149. doi:10.1038/ngeo2864

Nocquet, J.-M., Villegas-Lanza J.-C., Chlieh M., Mothes P.A., Rolandone F., Jarrin P., Cisneros D., Alvarado A., Audin L., Bondoux F., Martin X., Font Y., Regnier M., Vallée M., Tran T., Beauval C., Maguiña Mendoza J.M., Martinez W., Tavera H., Yepes H. (2014). Motion of continental slivers and creeping subduction in the northern Andes. Nat. Geosci. 7, 287_292.

Pararas-Carayannis G. (1980). Earthquake and Tsunami of 12 December 1979 in Colombia (International Tsunami Information Center, Honolulu).

Pararas-Carayannis, G. 1980: The Earthquake and Tsunami of December 12, 1979, in Colombia. Intern. Tsunami Information Center Report, Abstracted article in Tsunami Newsletter, Vol. XIII, No. 1.

Pararas-Carayannis, G., 2012: Potential of tsunami generation along the Colombia/Ecuador subduction margin and the Dolores-Guayaquil Mega-Thrust. Science of Tsunami Hazards, 31, 3: 209-230.

Ramírez J. (1958). Los terremotos de enero y febrero de 1958 en la costa del Pacífico de Ecuador y Colombia. Boletín de la Sociedad Geográfica de Colombia. Numero 58, vol. XVI.

Ratzov G, Sosson M, Collot JY, Migeon S (2012) Late quaternary geomorphologic evolution of submarine canyons as a marker of active deformation on convergent margins: the example of the South Colombian margin. Mar Geol 315–318:77–97

Reyes P, Michaud F., (2012) Mapa Geologico de la Margen Costera Ecuatoriana (1500000). EPPetroEcuador-IRD (eds), Quito, Ecuador

Robert G.P., Michetti A.M. (2004). Spatial and temporal variations in growth rates along active normal fault systems: an example from The Lazio – Abruzzo Apennines, central Italy. Journal of Structural Geology 26, 339-376.

Rodriguez, F., DHowitt, M.C., Toulkeridis, T., Salazar, R., Romero, G.E.R., Moya, V.A.R. and Padilla, O., 2016. The economic evaluation and significance of an early relocation versus complete destruction by a potential tsunami of a coastal city in Ecuador. Science of Tsunami Hazards, 35(1). 18-33.

Rudolph E, Szirtes S. (1911). "El terremoto colombiano del 31 de enero de 1906" Gerlands Beiträge zur Geophysik – Vol. XI, N° 1. Traducción: Hansjürgen Meyer, Alba de Cárdenas

Stirling M., Goded T., Berryman K., Litchfield N. (2013). Selection of earthquake scaling relationships for seismic-hazard analysis. Bulletin of the Seismological Society of America, Vol. 103, No. 6, pp. 2993-3011, doi: 10.1785/0120130052.

Toulkeridis T, Chunga K, Rentería W., Rodriguez F., Mato F., Nikolaou S., Antonaki N., Diaz-Fanas G., Cruz D´Howitt M, Besenzon D., Ruiz H., Parra H., Vera-Grunauer X. (2017). Mw7.8 Muisne, Ecuador 4/16/16 Earthquake observations: geophysical clustering, intensity mapping, Tsunami. 16th World Conference on Earthquake Engineering, 16WCEE 2017. Santiago Chile, January 9th to 13th 2017. Paper N° 5003. Registration Code: S-A1479327300

Toulkeridis, 2011: Volcanic Galápagos Volcánico. Ediecuatorial, Quito, Ecuador: 364 pp

Toulkeridis, T., Chunga, K., Rentería, W., Rodriguez, F., Mato, F., Nikolaou, S., Cruz D´Howitt, M., Besenzon, D., Ruiz, H., Parra, H. and Vera-Grunaer, X., 2017: The 7.8 M_w Earthquake and Tsunami of the 16th April 2016 in Ecuador - Seismic evaluation, geological field survey and economic implications. Science of Tsunami Hazards, in press

Trenkamp R, Kellogg JN, Freymueller JT, Mora P (2002) Wide plate margin deformation, southern Central America and northwestern South America, CASA GPS observations. J S Am Earth Sci 15:157–171

USGS (United States Geological Service), 2016: M7.8 - 29km SSE of Muisne, Ecuador. (http://earthquake.usgs.gov/earthquakes/eventpage/us20005j32#general)

USGS (United States Geological Service), 2017a: Historic Earthquakes, 1906 January 31st. (https://earthquake.usgs.gov/earthquakes/eventpage/official19060131153610_30#executive)

USGS (United States Geological Service), 2017b. M6.8 – near the coast of Ecuador. (https://earthquake.usgs.gov/earthquakes/eventpage/iscgem883714#executive)

USGS (United States Geological Service), 2017c. M7.7 – near the coast of Ecuador. (https://earthquake.usgs.gov/earthquakes/eventpage/usp00014ey#executive)

USGS (United States Geological Service), 2017d. Earthquakes Hazard Programm. (https://earthquake.usgs.gov/earthquakes/)

Veloza G., Styron R., Taylor M. (2012). Open-source archive of active faults for northwest South America. GSA Today, v. 22, no. 10, doi: 10.1130/GSAT-G156A.1.

Wells D. L. and Coppersmith K. J. (1994). New empirical relationships among magnitude, rupture length, rupture width, rupture area, and surface displacement: Bulletin of the Seismological Society of America, v. 84, p. 974-1002.

Wesnousky (2008). Displacement and geometrical characteristics of earthquake surface ruptures: issues and implications for seismic-hazard analysis and the process of earthquake rupture. Bulletin of the Seismological Society of America, Vol. 98, No. 4, pp. 1609-1632, doi: 10.1785/0120070111.

Wiens, D. A., & Stein, S. (1983). Age dependence of oceanic intraplate seismicity and implications for lithospheric evolution. *Journal of Geophysical Research: Solid Earth*, *88*(B8), 6455-6468.

Ye, L. Kanamori H., Avouac J.-P., Li L., Fai Cheung K., Lay T. (2016) The 16 April 2016, Mw 7.8 (Ms 7.5) Ecuador earthquake: a quasi-repeat of the 1942 Ms 7.5 earthquake and partial re-rupture of the 1906 Ms 8.6 Colombia_Ecuador earthquake. Earth Planet. Sci. Lett. 454, 248_258

Yepes, H., Audin, L., Alvarado, A., Beauval, C., Aguilar, J., Font, Y., Cotton, F. (2016): A new view for the geodynamics of Ecuador: implication in seismogenic sources definition and seismic hazard assessment. - Tectonics, 35, 5, pp. 1249—1279.

Yoshimoto M. Kumagai H., Acero W., Ponce G., Vasconez F., Arrais S., Ruiz M., Alvarado A., Pedraza Garcia P., Dionicio V., Chamorro O, Maeda Y., Nakano M. (2017). Depth-dependent rupture mode along the Ecuador-Colombia subduction zone. Geophysical Research Letters. 44, 2203-2210. Doi: 10.1002/2016GL071929.